Online dosimetry for temoporfin-mediated interstitial photodynamic therapy using the canine prostate as model.

Swartling, Johannes; Höglund, Odd V; Hansson, Kerstin; Södersten, Fredrik; Axelsson, Johan; Lagerstedt, Anne-Sofie

Published in:
Journal of Biomedical Optics

DOI:
10.1117/1.JBO.21.2.028002

2016

Journal of Biomedical Optics

BiomedicalOptics.SPIEDigitalLibrary.org

Online dosimetry for temoporfin-mediated interstitial photodynamic therapy using the canine prostate as model

Johannes Swartling
Odd V. Höglund
Kerstin Hansson
Fredrik Södersten
Johan Axelsson
Anne-Sofie Lagerstedt

SPIE.

Journal of Biomedical Optics 21(2), 028002 (February 2016)

Online dosimetry for temoporfin-mediated interstitial photodynamic therapy using the canine prostate as model

Johannes Swartling,[a,*] Odd V. Höglund,[b] Kerstin Hansson,[b] Fredrik Södersten,[c] Johan Axelsson,[d] and Anne-Sofie Lagerstedt[b]
[a]SpectraCure AB, Magistratsvägen 10, 226 43 Lund, Sweden
[b]Swedish University of Agricultural Sciences, Department of Clinical Sciences, Box 7054, Uppsala 750 07, Sweden
[c]Swedish University of Agricultural Sciences, Department of Biomedical Sciences and Veterinary Public Health, Box 7028, Uppsala 750 07, Sweden
[d]Lund University, Division of Atomic Physics, Physics Department, Box 118, Lund 221 00, Sweden

Abstract. Online light dosimetry with real-time feedback was applied for temoporfin-mediated interstitial photodynamic therapy (PDT) of dog prostate. The aim was to investigate the performance of online dosimetry by studying the correlation between light dose plans and the tissue response, i.e., extent of induced tissue necrosis and damage to surrounding organs at risk. Light-dose planning software provided dose plans, including light source positions and light doses, based on ultrasound images. A laser instrument provided therapeutic light and dosimetric measurements. The procedure was designed to closely emulate the procedure for whole-prostate PDT in humans with prostate cancer. Nine healthy dogs were subjected to the procedure according to a light-dose escalation plan. About 0.15 mg/kg temoporfin was administered 72 h before the procedure. The results of the procedure were assessed by magnetic resonance imaging, and gross pathology and histopathology of excised tissue. Light dose planning and online dosimetry clearly resulted in more focused effect and less damage to surrounding tissue than interstitial PDT without dosimetry. A light energy dose–response relationship was established where the threshold dose to induce prostate gland necrosis was estimated from 20 to 30 J/cm^2. [DOI: 10.1117/1.JBO.21.2.028002]

Keywords: photodynamic therapy; laser; mesotetrahydroxyphenylchlorin; prostate; dosimetry.

Paper 150757R received Nov. 6, 2015; accepted for publication Jan. 21, 2016; published online Feb. 17, 2016.

1 Introduction

Prostate cancer is one of the most common cancer forms in men.[1] Current radical treatments, which include surgery and radiotherapy, are associated with side effects primarily in the form of impotence and incontinence.[2]

Interstitial photodynamic therapy (PDT) is one alternative technique to treat prostate cancer.[3] The method relies on the use of a light activated drug, photosensitizer, and provides a minimally invasive treatment by the use of needles to insert optical fibers that guide the light to the target tissue. In addition, interstitial PDT potentially offers several other advantages: few side effects, rapid recovery, repeatable treatment if needed, and the method does not exclude other treatment options. Interstitial light delivery, in contrast to traditional PDT which utilizes surface illumination, allows treatment of voluminous tumors with complex structure inside the body.

The PDT mechanism involves formation of cytotoxic oxygen species.[4] In clinical trials of interstitial PDT, the outcome of the treatment has often been variable.[5] This may be due to limited control of local photosensitizer concentration,[6] the local light dose distribution in the tissue,[7] and unknown tissue oxygen concentration,[8] all of which may lead to variability in the generated dose of singlet oxygen. A key issue in the development of interstitial PDT for prostate cancer is to control the singlet oxygen dose and its distribution in the tissues, to ensure destruction of the malignant tissue while at the same time minimizing damage to surrounding organs. PDT treatment planning and dosimetry is largely a matter of controlling the light delivery. Several researchers have proposed adaptive dosimetry systems that monitor photosensitizer, oxygen concentration and light dose, and evaluate the light dose based on this input online.[9–12]

The development of the Lund system for interstitial PDT with online dosimetry has been described in a series of publications.[9,13–16] A unique feature of the system is that the same optical fibers are used for light delivery and measurements. The present version of the Lund system, the SpectraCure P18 system with IDOSE (Interactive Dosimetry by Sequential Evaluation), is adapted to temoporfin PDT of the prostate. The IDOSE software uses transrectal ultrasound images for light-dose planning of the prostate and surrounding tissues. The software computes optimum optical fiber positions, and once the fibers are in place, evaluates the optical measurements and computes the dose plan. The dosimetry is based on measurements of the local optical properties of the tissue (effective attenuation coefficient, μ_{eff}).

Clinically, PDT of prostate cancer has been performed in phase I/II studies using the photosensitizers padoporfin (WST-09),[3,17,18] padeliporfin (WST-11),[17,18] and motexafin lutetium.[19,20] In those studies, no or only limited PDT dosimetry

*Address all correspondence to: Johannes Swartling, E-mail: jsw@spectracure.com

1083-3668/2016/$25.00

was used, although image-based dose planning prior to the treatment was used in some cases.

Temoporfin (Foscan, mesotetrahydroxyphenylchlorin) has been used in conjunction with PDT of prostate, where no online dosimetry was used.[21,22] The SpectraCure P18 system has been used in a clinical study for treatment of low-risk localized prostate cancer, also with temoporfin.[23] The aim of the study was to show safety and feasibility of interstitial PDT of the prostate with online dosimetry. This was, to our knowledge, the first time online PDT dosimetry was used clinically. The results of the study highlighted that a key issue is to determine the correct threshold light dose to induce necrosis of the altered tissue. One of the main conclusions was that the target light dose was set too low to achieve ablation of the entire prostate.

Temoporfin-mediated PDT of dog prostate has been described by Chang et al.[24,25] The objectives were to investigate feasibility, study safety, and to determine light and drug dose parameters. In these studies, no attempt to ablate the entire prostate gland was made, and no PDT dosimetry was applied.

The purpose of the present study was to investigate the performance of online dosimetry in the dog prostate with temoporfin as photosensitizer. The study was designed to address the correlation between dose plans and tissue response, and the light energy dose needed to achieve necrosis of prostate tissue. Since the goal of the treatment was to create a necrotic region covering most of the prostate gland as result of the total light dose from multiple optical fibers, a key parameter for evaluation of the results was the light dose at the boundary of the necrotic region. This light dose can be interpreted as the threshold dose for necrosis to occur. The use of dog prostate allowed detailed evaluation of the effects of PDT by histopathological examination of the excised prostate gland and comparison with pre-PDT dose plans, an approach which is not feasible on human subjects.

2 Materials and Methods

2.1 *Photodynamic Therapy System and Dosimetry*

The system, SpectraCure P18 with IDOSE, was functionally similar to previously described instruments.[9,13,14] Eighteen individually controlled diode lasers, operating at 652 nm, were used as light sources; however, in the present study, only seven lasers were used because of the small size of the dog prostate. In monitoring mode, one fiber at a time was used as the emitter while the six closest surrounding fibers were used to collect and measure scattered light. With this setup, it was possible to monitor the optical properties of the tissue. The output power from each bare-end fiber was calibrated to 150 mW prior to each PDT session. Bare-end fibers were used because as point sources they provided both optimal light fluence measurement capability and a flexible means to shape the dose field.

A more detailed description of the dosimetry platform, IDOSE, is found in Refs. 15 and 16. Briefly, the three-dimensional (3-D) model of the prostate and surrounding tissues generated from transrectal ultrasound images was used as input for the calculation of optimum fiber positions, which were then presented to the user. Typical average optical properties of prostate tissue were used in the optimization, which was based on a stochastic method that positions the fibers in the 3-D prostate model with 2-mm spatial resolution, with constraints concerning organs at risk. All dose-related computations in IDOSE were based on the steady state diffusion equation of radiative transport; and thus, it was assumed that light propagation in the tissue takes place in the optically diffuse regime. When the optical fibers were in place the first monitoring sequence was performed. The optical properties were evaluated by assuming that the tissue was locally homogeneous around the seven optical fibers, where each fiber was sequentially used as emitter and the other fibers as receivers. The effective attenuation coefficient, μ_{eff}, was derived by fitting the data with the diffusion equation. The evaluated optical properties were used to compute a dose plan that was presented to the user, who then had to approve the start of the light delivery. The doses were determined by the illumination time of each fiber. The light delivery was interrupted at intervals for monitoring sequences, and the dose plan was updated in case significant changes had occurred. The dose planning algorithm aimed to deliver a minimum threshold light dose to all parts of the target volume, while attempting to avoid giving more than the threshold dose to surrounding organs at risk.

2.2 *Study Design*

The study had a sequential design in which groups of dogs were subjected to one threshold light dose. The results were evaluated, and the threshold dose was increased for the next group to a value based on the results of the previous group. In the first group, online dosimetry was not used, which allowed some comparison between the results when using online dosimetry and not using online dosimetry.

The study comprised nine clinically healthy intact male research Beagles, aged 15 to 33 months and weighing 14 to 20 kg. They were divided into three groups (three dogs in each group). They were housed at the Department of Clinical Sciences, Swedish University of Agricultural Sciences in Uppsala, Sweden. Food was provided once a day and water was freely available to the dogs. The dogs were observed daily by the same veterinarian to monitor the animals' general condition. Seven days after PDT, the dogs were euthanized with pentobarbital intravenously (IV) and subjected to autopsy.

The study was approved by the Uppsala Animal Ethics Committee, Sweden.

2.3 *Photodynamic Therapy*

Three days before PDT, temoporfin (Foscan, Biolitec Pharma, Jena, Germany), 0.15 mg/kg, was administered by slow IV injection in vena cephalica during a 10 min span. Following administration of temoporfin, the ambient light was subdued due to the photosensitivity caused by temoporfin.

The dogs were premedicated 30 to 40 min before induction of anesthesia with acepromazine (Plegicil vet, Pharmaxim, Helsingborg, Sweden) 0.3 mg/10 kg, administrated intramuscularly, and methadone (Metadon Recip, Solna, Sweden) 2 mg/10 kg, administrated subcutaneously.

Anesthesia was induced using propofol (Rapinovet vet, Schering-Plough A/S, Skovlunde, Denmark), administrated IV. After intubation, the anesthesia was maintained with isoflurane inhaled in 2% mixture of oxygen and air. All dogs breathed spontaneously.

When the animals were anesthetized, the surgical field ventral of the anus (i.e., perineum) was aseptically prepared. They were placed in the operating room in a dorsal recumbency. In order to create the desired angle of the pelvis for access to

the prostate, the dogs' hind legs were stretched cranially and medially and tied together ventrally to the mid-abdomen.

Transrectal ultrasound (2101 Falcon EXL, B-K Medical, Herlev, Denmark), frequency range 5 to 7.5 MHz, was used to acquire images of the prostate and surrounding organs, and to create a pretreatment dose plan. Seven 18-gauge needles were inserted according to the dose plan transperineally under ultrasound guidance. Once the needles with optical fibers were in place, light delivery and dosimetry were performed automatically by the SpectraCure P18 system without any user intervention except approval before the start of the light delivery. The light delivery was interrupted by the system for measurements after 2, 4, and 9 min, and then every 5 min for the duration of the treatment.

The number of fibers, 7, was chosen as the minimum number of fibers to acquire useful measurements for the online dosimetry. More fibers could not be used due to the small size of the prostate of the dogs.

2.4 *Light Threshold Dose*

The light threshold dose starting point was 5 J/cm^2, estimated from the lesion sizes reported by Chang et al.[24,25] In that study, typical lesion sizes resulting from PDT had radii of 9 to 11 mm for a light energy of 100 J (after selecting only the cases that were treated interstitially, were euthanized after 7 days, and showed clear, nonconfluent lesions from individual fibers). Assuming optical properties similar to human prostate,[26] this yields a threshold dose at the border of the lesions in the interval 3 to 18 J/cm^2. The value 5 J/cm^2 is in the lower end of this interval. This estimate was further verified by comparing with the recommended light dose for superficial illumination approved by the European Medicines Agency, 20 J/cm^2 (irradiance × illumination time). Assuming typical tissue optical properties and a depth of necrosis of 5 mm, this yields a threshold dose of 6 to 10 J/cm^2 (fluence), which is in the same range. [Note the distinction between the physical properties "irradiance" (to describe the light power incident on a surface) and "fluence rate" (to describe the light power per unit area at a location inside a turbid medium) although they have the same unit, W/cm^2.] Based on these two independent estimates, 5 J/cm^2 was chosen as a conservative starting point.

The first group of three dogs was given a fixed light energy of 63 J/fiber, which approximately corresponded to 5 J/cm^2 at the boundary of the prostate. Online dosimetry was used in the subsequent groups. After the results of group 1 had been evaluated, the 5-J/cm^2 level was clearly too low to achieve the aim of ablating the entire prostate, and the target threshold dose was set to 10 J/cm^2 for group 2. Dog 6 was used as a control and received temoporfin and was subjected to fiber insertion but no light. The target threshold dose was finally increased to 20 J/cm^2 for the third group, based on the observation that even the 10 J/cm^2 target threshold used for the second group was not enough to achieve total ablation of the prostate.

2.5 *Magnetic Resonance Imaging*

The dogs were premedicated with dexmedetomidin (Dexdomitor, Orion Pharma Animal Health, Sollentuna, Sweden) 0.3 mg/kg and butorfanol (Dolorex vet, Intervet, Stockholm, Sweden) 0.2 mg/kg.

Magnetic resonance imaging (MRI) of the prostate was performed before administration of temoporfin and on day 7 after PDT. The dogs were examined in lateral recumbency in a 0.27 T permanent, C-shaped magnet (Hallmarq Veterinary Imaging, Guildford, United Kingdom). The sequences were T1-weighted spin echo (T1W SE) pre- and postcontrast and T2-weighted fast spin echo (T2W FSE). For the contrast examination, each dog received 0.2 mL/kg gadodiamid (Omniscan, GE Healthcare, Chalfont St. Giles, United Kingdom) administered by IV injection. Directly after the second MRI examination, the dogs were euthanized with pentobarbital IV and subjected to autopsy.

2.6 *Histopathology*

At necropsy, the prostate, adjacent rectum and bladder was measured and weighed and then fixed in 10% neutral buffered formalin. For macroscopic inspection, the prostate tissue was sectioned from the cranial part to the caudal end in 4- to 6-mm thick blocks transversally cut. Each block was evaluated macroscopically and then embedded in paraffin. Sections (5- to 7-μm thick) from each block were processed for histological examination using hematoxylin and eosin staining and van Gieson staining. Tissues adjacent to the prostate, i.e., the bladder and colon, were collected and processed for histological examination.

2.7 *Blood Sampling*

Blood samples were collected from all animals before administration of temoporfin and at ~1, 3, 6, 24, 48, and 72 h postadministration. The samples were shipped on dry ice for high-performance liquid chromatography (HPLC) analysis by Biolitec AG, Germany.

3 Results

Online dosimetry was used in groups 2 and 3, but not group 1, where the dogs instead received fixed light energy of 63 J/fiber. This allowed comparison of PDT with and without online dosimetry.

All dogs appeared less active than normally the first day after the PDT treatment, but their intake of food and water was normal. One of the dogs (dog 7) had difficulty in urinating 2 days after treatment. The urine was removed through a catheter until the dog was euthanized at day 7. He was treated with carprofen 4 mg/kg s.c. (Rimadyl vet, Orio Pharma Animal Health, Stockholm) for 5 days. In the other eight dogs, the general condition was considered normal from the second day until they were euthanized.

All images in this section are presented according to radiological convention, with the ventral part of the prostate up.

3.1 *Gross Pathology and Histopathology*

Within the prostate tissue, there were changes of various degree and location in all dogs except dog 6 (control). Dogs 1, 2, 3, and 9 had lesions characterized by hemorrhages in the interstitium and only a few small necrotic foci within the prostate parenchyma. These necrotic areas were located in the center of the hemorrhagic zones. In dogs 4 and 5, several foci of necrosis ranging from a few mm up to 13 mm in diameter were found. Figures 1(a)–1(c) illustrate an example from dog 4. These necrotic areas were surrounded by hemorrhagic zones that in many areas extended into the capsule. In dogs 7 and 8, large necrotic lesions were found in the glandular and interstitial parts

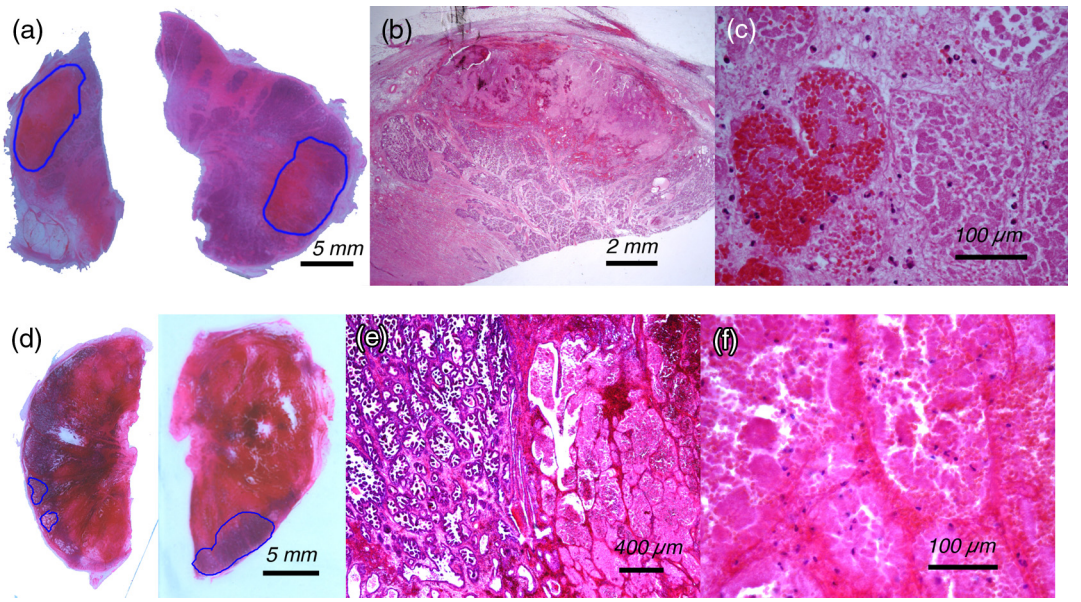

Fig. 1 Necrotic areas and lesions. (a) Transverse slices from dog 4. The contours denote the regions of necrosis. (b and c) Dog 4. H&E-stained histological slides. (b) Low magnification shows large necrotic areas with hemorrhages that extend into the capsule. (c) High magnification, illustrating coagulation necrosis with hemorrhages and only few inflammatory cells. (d) Transverse slices from dog 7. The contours denote the remaining regions of healthy tissue. (e and f) Dog 7, H&E stained histological slides. (e) Low magnification, illustrating a distinct border between the necrotic areas to the right and the viable glandular tissue to the left. (f) High magnification, coagulation necrosis with hemorrhages and few inflammatory cells.

of the prostate. Figures 1(d)–1(f) show an example from dog 7. These lesions were surrounded by hemorrhagic zones.

In all dogs except dog 6 (control), there were changes in the prostate capsule and the periprostatic tissue. These changes were characterized by hemorrhages, edema and necrosis of fat and loose connective tissue. In addition, there were fibrin accumulation and inflammatory cells (mainly lymphocytes and macrophages) admixed with few fibroblasts in these areas.

Dogs 1, 2, 3, and 7 had multifocal petechial hemorrhages in the urinary bladder mucosa. In the rectum/colon part, direct dorsally of the prostate lesions were found in dogs 1, 3, 7, 8, and 9. These lesions included necrosis of mucosal, submucosal, and muscular layers with vasculitis and thrombosis. Comparison of metric data before and after paraffin embedding showed that the shrinkage of the tissue was between 5% and 8%.

3.2 *Magnetic Resonance Imaging*

Multiple intensity changes were seen in post-PDT scans both in the prostatic and the periprostatic tissues. All dogs showed similar intensity changes in the prostate compared to pre-PDT with a diffuse mixed intensity in T1W SE, marked contrast enhancement in T1W SE, and slight to moderate hyperintensity compared to surrounding fat in T2W FSE scans. The changes were generally distributed in the prostate in dogs 1 to 3 and 7 to 9, whereas dogs 4 and 5 had focal changes. See Fig. 2 for examples from dogs 4 and 7.

Areas of signal void in contrast-enhanced T1W SE scans were seen in dogs 1 (small focal area), 2 (three small focal areas), 4 (two large areas), 5 (two large areas), 7 and 8 (multiple large areas). No areas of signal void were seen in dogs 3 and 9.

In all dogs that had PDT, the prostatic capsules were irregular and diffuse in outline and the periprostatic fatty tissue contained multiple irregular hypointense linear structures. Dogs 1, 3, 7, and 8 also had semicircular areas of signal void in contrast-enhanced T1W SE scans along the periphery of the right prostatic lobe [see Fig. 2(e)].

Similar intensity changes in the ventral rectum were seen in dogs 1, 3, and 9, which were hypointense in T1W SE, hyperintense in T2W FSE and showed signal void in contrast-enhanced T1W SE scans. The border of the rectal lesion gradually became indistinguishable and on scans cranial to the lesion, it was not possible to distinguish between intensity changes in the periprostatic tissue and the lesion in the rectal wall. Dog 8 showed contrast enhancement in the ventral rectal wall and nearby muscular tissue but no signal void.

3.3 *Dosimetry*

The performance of the dosimetry was assessed by analysis of light dose plans and measurement data. Isodose maps were calculated based on measurements and delivered light doses. The isodose maps were two-dimensional plots representing transverse slices taken from the tissue 3-D model, where isodoses represented the areas of the tissue that received above or below certain levels of light fluence dose. The isodose maps were compared with the pathology results to determine the light dose level at which tissue necrosis occurred. The dose maps were rescaled to fit the pathology slides to account for the shrinking of the tissue. The transverse planes were coregistered with the histopathology samples by observing the position of the histopathology cut in relation to the cranial and caudal ends, and selecting the corresponding plane in the 3-D tissue model.

As previously noted, in dogs 1 to 3, the online dosimetry was not active. Instead, a fixed light energy of 63 J/fiber was

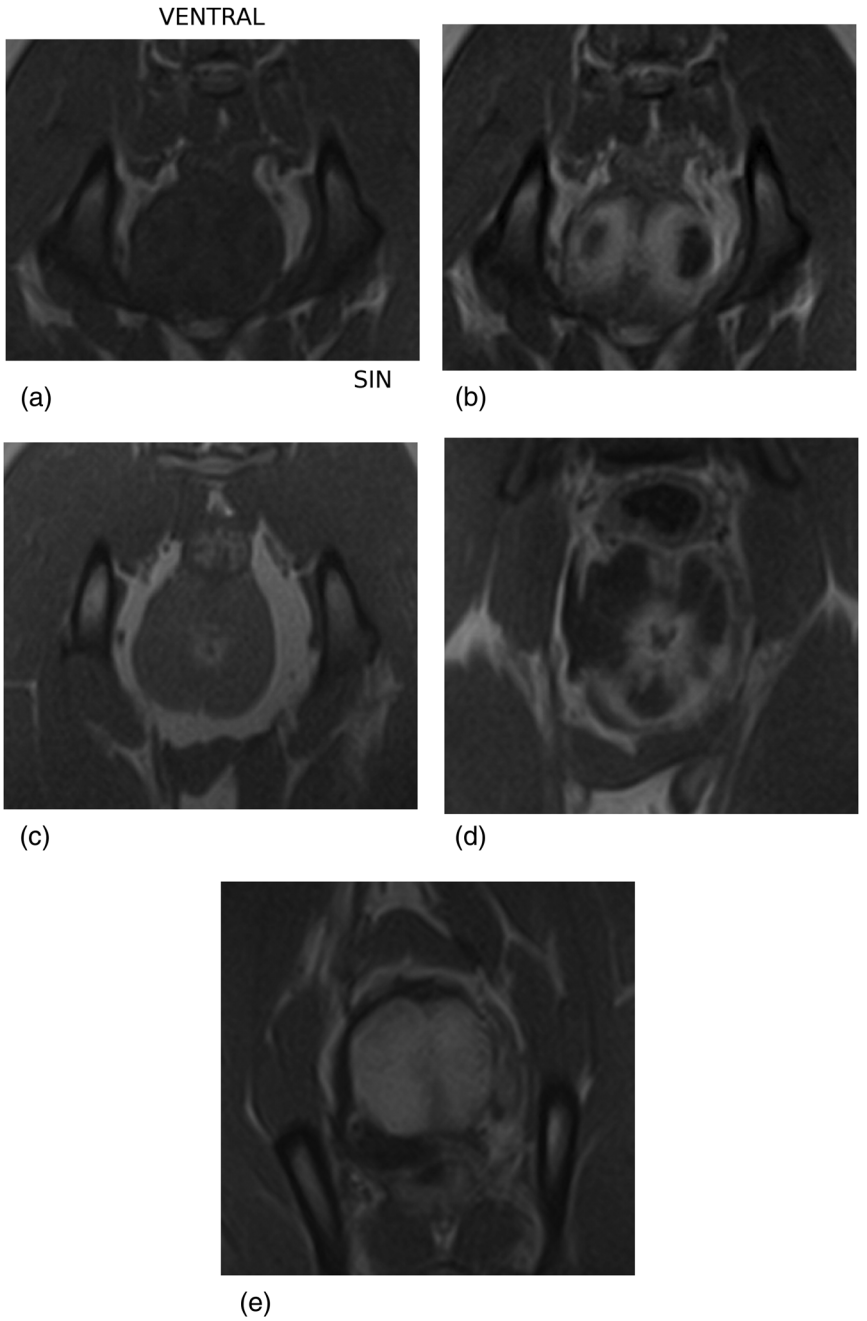

Fig. 2 Magnetic resonance T1W SE images (time to echo 18 ms, time to repetition 400 ms) of (a, b) dog 4, (c, d) dog 7, and (e) dog 3. (a and b) Dog 4, post-PDT. The precontrast image shows areas of mixed intensity in both left and right prostatic lobes that in postcontrast scans (b) are hyperintense with semicircular areas of signal void. (c and d) Magnetic resonance T1W SE contrast-enhanced images of dog 7 pre- and post-PDT. (d) The post-PDT image shows changes in the entire prostate with hyperintense parenchyma surrounding large areas of signal void. (e) Magnetic resonance T1W SE contrast-enhanced image of dog 3 post-PDT. Semicircular area of signal void representing hemorrhages and necrosis surrounds the right prostatic lobe. No areas of signal void in the prostatic tissue. SIN: sinister, left.

delivered. Post-PDT analysis based on the measurements was performed, and light dose maps were reconstructed and compared with the histopathology results. This comparison indicated that the light dose at the perimeter of the necrotic regions was ~20 to 30 J/cm^2.

In dogs 4, 5, 7–9, the online dosimetry was active. Examples of the resulting dose maps for dogs 4 (threshold dose 10 J/cm^2) and 7 (threshold dose 20 J/cm^2) are shown in Fig. 3. The dose maps were compared with the histopathology results [cf. Figs. 1(a) and 1(d) for dogs 4 and 7, respectively]. This again was consistent with a threshold dose to induce necrosis of ~20 to 30 J/cm^2, in all dogs except in dog 9, where the light dose needed to achieve necrosis was much higher at over 100 J/cm^2. There was no obvious difference between dog 9 and the other dogs from a dosimetry perspective, except that the prostate in dog 9 was smaller.

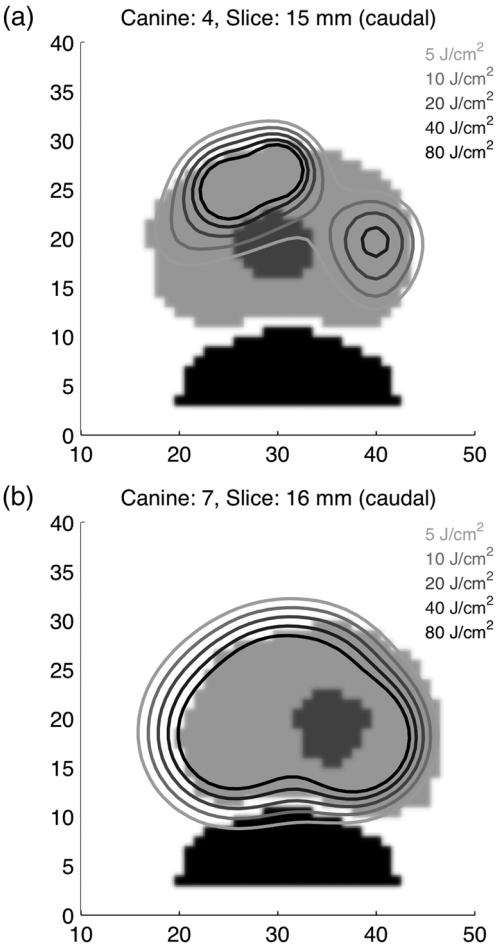

Fig. 3 Dose maps from (a) dog 4 and (b) dog 7, corresponding to the same transverse slices, as shown for the histopathology in Fig. 1. Axes scale: mm. Tissue model: light gray—prostate; medium gray—urethra; dark gray—rectum.

The light illumination times and delivered light doses are shown in Table 1, where t_{min} denotes the shortest illumination time of the seven fibers, $t_{average}$ the average time, and t_{long} the longest. The total light dose delivered to each dog is also shown. The measured effective attenuation coefficients, μ_{eff}, of the prostate tissue are presented in Fig. 4. For each dog, the average μ_{eff} value for every monitoring sequence is shown together with the standard deviation. The interfiber distances were in the range of 5 to 25 mm in all cases.

Dose–volume histograms for dogs 4 and 7 are shown in Fig. 5, as examples from one dog in group 2 and one in group 3. As a summary of the results for all dogs, the percentage volume of prostate tissue that received the target threshold dose is shown for all dogs in Fig. 6.

3.4 *Pharmacokinetics*

All plasma samples were investigated by HPLC analysis to specify the temoporfin content. The maximum plasma concentration in all animals was ~0.6 ng temoporfin/mg wet weight, measured 1 h after injection. The average elimination half-life of temoporfin was 18 h. This value is similar to that reported in dogs by Buchholz et al.[27]

Table 1 PDT illumination times and light doses.

Dog	Target threshold dose (J/cm^2)	t_{short} (min)	$t_{average}$ (min)	t_{long} (min)	Total light dose (J)
1	—	7.0	7.0	7.0	441
2	—	7.0	7.0	7.0	441
3	—	7.0	7.0	7.0	441
4	10	1.2	5.0	10.0	315
5	10	0.1	4.2	9.7	265
6	—	—	—	—	0
7	20	1.9	15.7	20.0	989
8	20	0.2	6.0	12.4	378
9	20	0.9	7.9	16.9	498

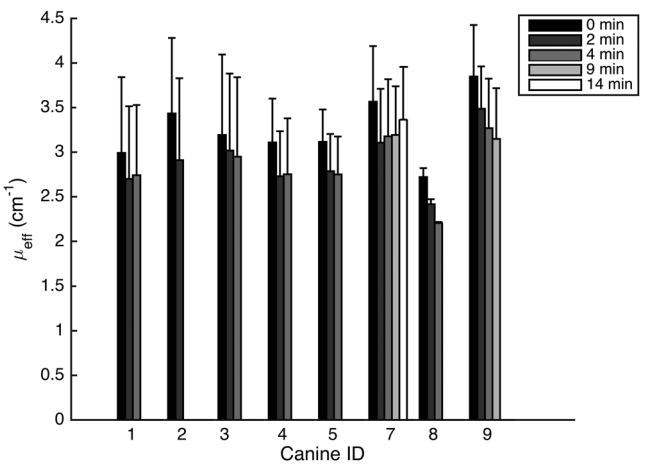

Fig. 4 The average effective attenuation coefficient at different monitoring times during PDT for each dog. The average and standard deviation of the effective attenuation coefficient at each monitoring time is calculated from the unique values of effective attenuation coefficient for each treatment fiber as assessed by the PDT instrument during therapy.

4 Discussion

The purpose of the study was to investigate the correlation between dose plans and tissue response, and the light energy dose needed to achieve necrosis of prostate tissue. The intention was to intervene the healthy canine prostate in the same manner, to the extent that it was possible, as in the case of clinical treatment of prostate cancer, with the aim to ablate the entire prostate gland using PDT.

In dogs 1 to 3, necrosis and hemorrhages were seen relatively extensively in the rectum, bladder, and periprostatic tissue, which shows that the intervention was not particularly specific to the prostate in this group. This is most likely due to the fact that online dosimetry was not used; optical fibers that were placed close to the prostate border delivered a substantial dose to surrounding tissues. Despite the damage to surrounding organs, the dogs did not express severe clinical symptoms during the 1-week follow up.

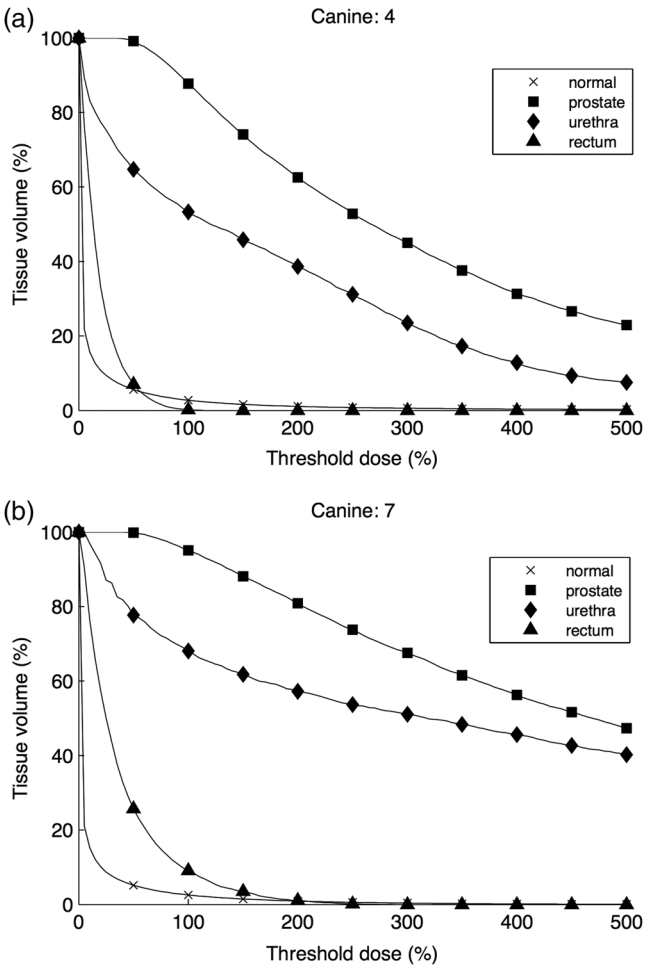

Fig. 5 Dose–volume histograms for (a) dog 4 and (b) dog 7. The threshold dose was set at 10 J/cm^2 for dog 4 and 20 J/cm^2 for dog 7.

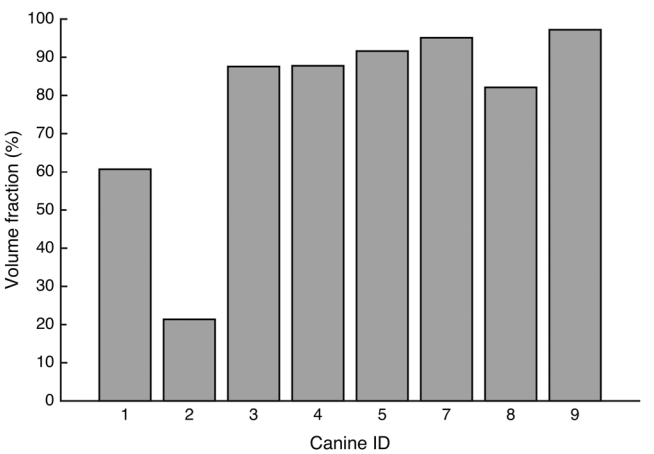

Fig. 6 The volume fraction of the prostate that received the target threshold dose for all dogs.

Based on the registered measurement data, it was possible to reconstruct dose maps for dogs 1 to 3, and compare these with the pathology results. This comparison gave an estimated threshold dose of 20 to 30 J/cm^2 to induce necrosis.

The results for dogs 1 to 3 serve as a benchmark for interstitial PDT without the use of online dosimetry. It is clear that delivery of a fixed light energy per fiber (in this case 63 J/fiber) was not a successful approach to reach the objective. Tissue changes were seen outside the prostate, including both rectum and bladder, and the changes within the prostate were scattered and nonfocused.

The overall results from dogs 4 to 9 are a clear indication that dose planning and online dosimetry led to improved results, both in terms of focusing the PDT effect to the target volume and to achieve the objective of attaining the threshold dose to induce necrosis. The dose volume histograms (Fig. 5) show that almost complete coverage of the target prostate tissue was attained by the dose-planning algorithm. Note that this does not mean that complete response in the volume is expected, since the threshold dose needed for tissue necrosis was unknown *a priori*.

The measured optical properties are similar in range to those measured in human prostate with the SpectraCure P18 system,[23] and also in the same range as those reported for human prostate in other studies.[26]

The threshold dose was estimated by comparing the isodose maps with the extension of the necrotic lesions seen in the histopathology. Some degree of uncertainty arises due to the fact that perfect colocalization between isodose maps and histopathology samples was not possible. The prostate may have changed during the 7-day period between PDT and euthanasia, and the shape of the organ may have been distorted differently. The colocalization error may be in the order of a few millimeters. It should also be noted that the PDT threshold model is simplified, since variations in the local photosensitizer concentration and oxygen concentration are not taken into account.

Dogs 4 and 5 were clearly undertreated as seen from the goal to achieve necrosis in the entire target region. Dog 6 (control) did not exhibit any histopathological changes, which shows that photosensitizer and needle trauma alone resulted in negligible effect.

Dogs 7 and 8 responded with large necrotic lesions in the target region, which indicates that the target threshold dose of 20 J/cm^2 was close to the dose needed to achieve total ablation. By contrast, dog 9 only had small lesions despite being subjected to the same target threshold dose. Dog 9 had a smaller prostate than dogs 7 and 8, but the reason behind the lower PDT effect is unknown. The plasma samples did not reveal a difference in temoporfin concentration for dog 9.

The threshold dose to induce necrosis was estimated from 20 to 30 J/cm^2 in all dogs except dog 9 (and the control), based on tissue necrosis found in the histopathological examination. However, there was always a large zone of hemorrhaging and inflammation surrounding the necrosis. It is not clear how these changes develop over a longer time than the 1-week follow up used in this study. Even though the results from this study point to a threshold dose of 20 to 30 J/cm^2 in dog prostate, this result may not necessarily be directly transferrable to the case of human prostatic tissue. Nevertheless, the outcome of the clinical trial indicated that the target dose of 5 J/cm^2 used in that study was too low,[23] and the results from this study support the use of higher light doses in future clinical trials.

Changes in the rectum and bladder were seen in dogs 1 to 3 and 7 to 9, however, less severe in dogs 7 to 9. The significance of these changes is not entirely clear. The animals seemed largely unaffected during the 1-week follow up. In superficial PDT with temoporfin, it is common to see extensive tissue damage even extending outside the target area, which usually heals

remarkably well.[28] Dog 9 exhibited changes to rectum and bladder despite having only minor necrotic lesions in the prostate itself, which leads to the question whether prostate glandular tissue is more resistant to PDT than the surrounding tissues.

To summarize, light-dose planning and online dosimetry using SpectraCure P18 with IDOSE resulted in more focused PDT effect and less damage to surrounding tissue than interstitial PDT without dosimetry. A light dose–response relationship was established where the threshold dose to induce prostate gland necrosis was estimated to be in the interval 20 to 30 J/cm^2. Dose planning with a target dose of 20 J/cm^2 in the target volume led to changes to rectum and bladder, however, the significance of which is unclear. The results from this study, together with the results from previous the clinical study,[23] support the use of target dose levels higher than 5 J/cm^2 in future clinical studies of temoporfin-induced prostate PDT.

Acknowledgments

We express our appreciation to the late Dr. Ann Johansson, whose contribution to this work was of great significance. We thank Biolitec AG for providing Foscan and Stephan Dymling for technical assistance. This work was funded by SpectraCure AB.

References

1. A. Jemal et al., "Cancer statistics," *CA Cancer J. Clin.* **57**, 43–66 (2007).
2. C. Parker et al., "A model of the natural history of screen-detected prostate cancer, and the effect of radical treatment on overall survival," *Br. J. Cancer* **94**, 1361–1368 (2006).
3. C. M. Moore, D. Pendse, and M. Emberton, "Photodynamic therapy for prostate cancer—a review of current status and future promise," *Nat. Clin. Pract. Urol.* **6**, 18–30 (2009).
4. K. R. Weishaupt, C. J. Gomer, and T. J. Dougherty, "Identification of singlet oxygen as the cytotoxic agent in photoinactivation of a murine tumor," *Cancer Res.* **36**, 2326–2329 (1976).
5. W. Jerjes et al., "Ultrasound-guided photodynamic therapy for deep seated pathologies: prospective study," *Lasers Surg. Med.* **41**, 612–621 (2009).
6. X. D. Zhou et al., "Pretreatment photosensitizer dosimetry reduces variation in tumor response," *Int. J. Radiat. Oncol. Biol. Phys.* **64**, 1211–1220 (2006).
7. J. Li and T. C. Zhu, "Determination of in vivo light fluence distribution in a heterogeneous prostate during photodynamic therapy," *Phys. Med. Biol.* **53**, 2103–2114 (2008).
8. T. M. Busch et al., "Photodynamic therapy creates fluence rate-dependent gradients in the intratumoral spatial distribution of oxygen," *Cancer Res.* **62**, 7273–7279 (2002).
9. T. Johansson et al., "Feasibility study of a system for combined light dosimetry and interstitial photodynamic treatment of massive tumors," *Appl. Opt.* **41**, 1462–1468 (2002).
10. M. D. Altschuler et al., "Optimized interstitial PDT prostate treatment planning with the Cimmino feasibility algorithm," *Med. Phys.* **32**, 3524–3536 (2005).
11. B. C. Wilson, M. S. Patterson, and L. Lilge, "Implicit and explicit dosimetry in photodynamic therapy: a new paradigm," *Laser Med. Sci.* **12**, 182–199 (1997).
12. R. A. Weersink et al., "Techniques for delivery and monitoring of TOOKAD (WST09)-mediated photodynamic therapy of the prostate: clinical experience and practicalities," *J. Photochem. Photobiol. B* **79**, 211–222 (2005).
13. A. Johansson et al., "System for integrated interstitial photodynamic therapy and dosimetric monitoring," *Proc. SPIE* **5689**, 130 (2005).
14. M. Soto-Thompson et al., "Clinical system for interstitial photodynamic therapy with combined on-line dosimetry measurements," *Appl. Opt.* **44**, 4023–4031 (2005).
15. A. Johansson et al., "Realtime light dosimetry software tools for interstitial photodynamic therapy of the human prostate," *Med. Phys.* **34**, 4309–4321 (2007).
16. A. Johansson et al., "Interstitial photodynamic therapy for primary prostate cancer incorporating real-time treatment dosimetry," *Proc. SPIE* **6427**, 64270O (2007).
17. J. Trachtenberg et al., "Vascular-targeted photodynamic therapy (padoporfin, WST09) for recurrent prostate cancer after failure of external beam radiotherapy: a study of escalating light doses," *BJU Int.* **102**, 556–562 (2008).
18. N. Arumainayagam et al., "Photodynamic therapy for focal ablation of the prostate," *World J. Urol.* **28**, 571–576 (2010).
19. K. Verigos et al., "Updated results of a phase I trial of motexafin lutetium-mediated interstitial photodynamic therapy in patients with locally recurrent prostate cancer," *J. Environ. Pathol. Toxicol. Oncol.* **25**, 373–387 (2006).
20. H. Patel et al., "Motexafin lutetium-photodynamic therapy of prostate cancer: short- and long-term effects on prostate-specific antigen," *Clin. Cancer Res.* **14**, 4869–4876 (2008).
21. T. R. Nathan et al., "Photodynamic therapy for prostate cancer recurrence after radiotherapy: a phase I study," *J. Urol.* **168**, 1427–1432 (2002).
22. C. M. Moore, T. R. Nathan, and W. R. Lees, "Photodynamic therapy using meso tetra hydroxy phenyl chlorin (mTHPC) in early prostate cancer," *Lasers Surg. Med.* **38**, 356–363 (2006).
23. J. Swartling et al., "System for interstitial photodynamic therapy with online dosimetry: first clinical experiences of prostate cancer," *J. Biomed. Opt.* **15**, 058003 (2010).
24. S. C. Chang et al., "Interstitial and transurethral photodynamic therapy of the canine prostate using meso-tetra-(m-hydroxyphenyl) chlorine," *Int. J. Cancer* **67**, 555–562 (1996).
25. S. C. Chang, I. F. Y. Chern, and Y. H. Hsu, "Biological response of dog prostate and adjacent structures after meso-tetra-(m-hydroxyphenyl) chlorin and aluminum disulfonated phthalocyanine based photodynamic therapy," *Proc. Natl Sci. Counc. ROC (B)* **23**, 158–166 (1999).
26. T. Svensson et al., "*In vivo* optical characterization of human prostate tissue using near-infrared time-resolved spectroscopy," *J. Biomed. Opt.* **12**, 014022 (2007).
27. J. Buchholz et al., "Optimizing photodynamic therapy: *in vivo* pharmacokinetics of liposomal meta-(tetrahydroxyphenyl)chlorin in feline squamous cell carcinoma," *Clin. Cancer Res.* **11**, 7538–7544 (2005).
28. K. F. M. Fan et al., "Photodynamic therapy using mTHPC for malignant disease in the oral cavity," *Int. J. Cancer* **73**, 25–32 (1997).

Johannes Swartling received his PhD in physics from Lund University (2002). He has worked with product development and general management in the medical device company SpectraCure AB since 2006. Before joining SpectraCure AB, he held postdoctoral research positions at Politecnico di Milano, Italy, and at Cambridge University, United Kingdom. His research has been on applications of laser technology and spectroscopy in biology and medicine.

Odd V. Höglund has worked with the development and clinical tests of resorbable implants in veterinary surgery, aimed to enable an easier and safer surgery. New surgical techniques are continuously being developed. Objective methods are needed for evidence-based comparison and evaluation. In his research he has focused on intraoperative measurements of surgical stress in veterinary surgery.

Kerstin Hansson has been a licensed veterinarian since 1984, working with veterinary diagnostic imaging since graduation. Formal specialization in diagnostic imaging includes Swedish (2006) and British (1992) degrees. She has been a European Diplomate of the European College of Veterinary Diagnostic Imaging since 2006. She received her PhD on imaging of cardiopulmonary structures in dogs in 2004. She is a associate professor in veterinary diagnostic imaging (2008) at the Swedish University of Agricultural Sciences. She works with small and large animals and all imaging.

Fredrik Södersten is a doctor in veterinary medicine and veterinary pathology. He has worked with extracellular and morphological changes in injured equine tendons with special interest in morphometry. As a diagnostic pathologist he has been involved in several

different research projects evaluating morphological changes related to either specific diseases or to post-surgical changes.

Johan Axelsson received his PhD in atomic physics from Lund University in 2010, after defending the thesis "Model-based approaches to diffuse optical imaging and dosimetry." During 2010-2011 he was appointed by Thayer School of Engineering, Dartmouth College, as a research associate. From 2011 he has been a member of the biophotonics group at Atomic Physics, managing projects involving molecular imaging of treatment response following targeted radionuclide therapy.

Anne-Sofie Lagerstedt is a senior professor in small animal surgery. She is still involved in several surgical research projects, for example, "Biomarkers for stress and pain assessment in companion animals" and "Development of a new implant and method for the treatment of focal full thickness cartilage lesions of the knee."